

Electrocatalysis

International Edition: DOI: 10.1002/anie.201701280
German Edition: DOI: 10.1002/ange.201701280**Oxygen-Incorporated Amorphous Cobalt Sulfide Porous Nanocubes as High-Activity Electrocatalysts for the Oxygen Evolution Reaction in an Alkaline/Neutral Medium**Pingwei Cai⁺, Junheng Huang⁺, Junxiang Chen, and Zhenhai Wen^{*}

Abstract: A novel OER electrocatalyst, namely oxygen-incorporated amorphous cobalt sulfide porous nanocubes (A-CoS_{4.6}O_{0.6} PNCs), show advantages over the benchmark RuO₂ catalyst in alkaline/neutral medium. Experiments combining with calculation demonstrate that the desirable O* adsorption energy, associated with the distorted CoS_{4.6}O_{0.6} octahedron structure and the oxygen doping, contribute synergistically to the outstanding electrocatalytic activity.

Development of renewable power sources (for example, sunlight and wind) is a promising strategy to minimize the negative consequences caused by the consumption of fossil fuels. Accordingly, a variety of energy conversion techniques,^[1] such as water splitting, CO₂ reduction, and metal–air batteries, have received more and more attention owing to their great potential for lessening the burden of energy demand. The oxygen evolution reaction (OER), as one key reaction involved in various energy-conversion systems, has been widely studied in recent years.^[2] However, the development of efficient electrocatalysts toward OER still remains a daunting challenge, because OER electrocatalysts suffer dramatically from high overpotential and poor durability. Up to now, the most efficient electrocatalysts for OER are Ir- and Ru-based materials,^[3] but the high cost of such noble-metal catalyst greatly impedes their large-scale applications. Hence, it is highly desirable to develop high-activity and noble-metal free OER catalysts with wider flexibility.

Over the past years, tremendous efforts have been devoted to developing earth-abundant materials as OER catalysts. It is well documented that the activity and durability of an electrocatalyst highly depend on its microscopic, crystalline, and dimensional structure.^[4] Transition metal (oxy)hydroxides^[5] and some layered double hydroxides materials^[6] have been extensively studied owing to their attractive OER activity, especially in alkaline solution. However, the natural feature of these metal hydroxides (or

oxides) make them behave unstable at low pH.^[7] Furthermore, transition-metal dichalcogenides (TMDs) have been extensively applied as the electrocatalysts for hydrogen evolution reaction,^[8] while the OER activity of the TMDs is still unsatisfactory. Recently, Xie et al. reported that the catalytic activity for OER on metal sulfides can be significantly improved by tuning the structure of electronic states by generating exposed octahedral planes in ultrathin nanosheets.^[9] Also, the distorted octahedral structure is identified as active sites for OER.^[4e,10] Based on this point, constructing a catalyst with plentiful disorder metal–sulfur octahedron is highly prospective for acquiring high activity for OER. Furthermore, amorphous materials usually have isotropic properties with largely locally disordered structure,^[11] which enable a mass of distorted octahedral structure to come into being in transition-metal sulfides. Furthermore, heteroatom (for example, nitrogen, oxygen, sulfur) doping has been widely used to enhance the activity sites and conductivity for promoting catalytic activity.^[12]

Bearing these points in mind, herein we propose a facile strategy for synthesis of oxygen-incorporated amorphous CoS_x porous nanocubes (A-CoS_{4.6}O_{0.6} PNCs), which was implemented by ionic exchange reaction on Prussian Blue Analogue (PBA) with S²⁻ replacing Fe(CN)₆³⁻. The anionic exchange reaction endows the A-CoS_{4.6}O_{0.6} PNCs with porous structure consisting of a large amount of defect sites. Moreover, the A-CoS_{4.6}O_{0.6} PNCs tend to generate more active Co–S dangling bond with introducing oxygen into host, dramatically strengthening the O* adsorption that can promote water oxidation reaction with high activity.

For preparing A-CoS_{4.6}O_{0.6} PNCs, crystalline Co-Fe PBA with a well-defined nanocubic structure was prepared and was used as precursor, followed by galvanic replacement reaction with Na₂S and subsequent calcination at 300 °C for 1 h under an Ar atmosphere (Figure 1a). Field-emission scanning electron microscopy (FESEM) images show that the as-synthesized Co-Fe PBA nanocubes are homogeneous distribution with an average size of about 360 nm (Figure 1b; Supporting Information, Figure S1), which is basically consistent with the previous work.^[13] The peaks on the XRD pattern of the Co-Fe PBA (Supporting Information, Figure S2) are well assigned to the cubic Co₃[Fe(CN)₆]₂·(H₂O)₁₇.

After galvanic replacement reaction, the obtained products, that is, the A-CoS_{4.6}O_{0.6} PNCs well maintain the frame and morphology of the Co-Fe PBA with decreasing the cube size to about 260 nm (Figure 1c,d). Interestingly, the A-CoS_{4.6}O_{0.6} PNCs show much coarser in plane surfaces than the Co-Fe PBA. A close observation reveals that the A-CoS_{4.6}O_{0.6} PNCs were actually composed of abundant ultrafine nano-

[*] P. W. Cai,^[†] Dr. J. H. Huang,^[†] Dr. J. X. Chen, Prof. Z. H. Wen
CAS Key Laboratory of Design and Assembly of Functional Nanostructures, Fujian Institute of Research on the Structure of Matter, Chinese Academy of Sciences
Fuzhou, Fujian 350002 (P.R. China)
and
Fujian Provincial Key Laboratory of Nanomaterials, Fujian Institute of Research on the Structure of Matter, Chinese Academy of Sciences
Fuzhou, Fujian 350002 (P.R. China)
E-mail: wen@fjirsm.ac.cn

[†] These authors contributed equally to this work.

Supporting information for this article can be found under:
<http://dx.doi.org/10.1002/anie.201701280>.

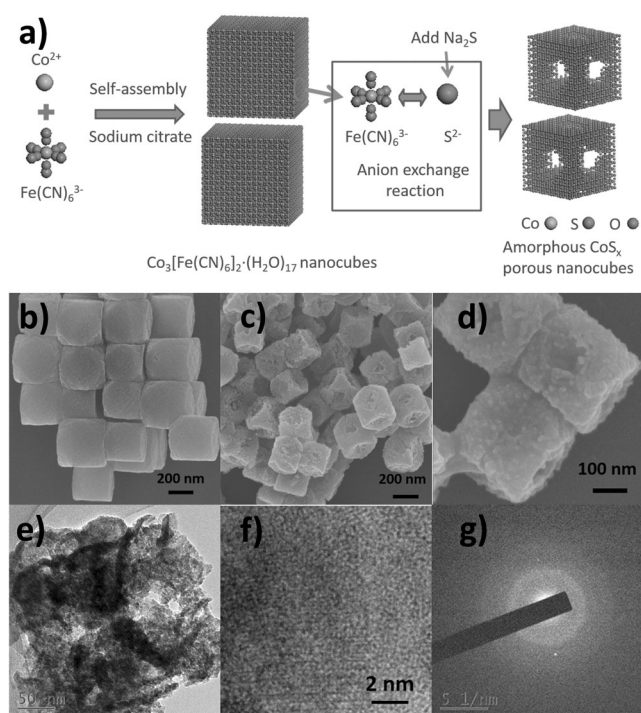


Figure 1. a) Illustration of synthesized process of A-CoS_{4.6}O_{0.6} PNCs; b) SEM image of Co-Fe PBA precursor; c), d) SEM images at different magnification; e) corresponding TEM image; f) high-resolution TEM image; g) SAED pattern of A-CoS_{4.6}O_{0.6} PNCs.

particles. Furthermore, the cubic structure shrinks inward with forming a lot of cavities, as manifested by the TEM images (Figure 1 e). There is no obvious diffraction peak on the XRD pattern of the A-CoS_{4.6}O_{0.6} PNCs (Supporting Information, Figure S3), suggesting that the sample is amorphous. The amorphous structure for the A-CoS_{4.6}O_{0.6} PNCs is further proved by high-resolution transmission electron microscopy (HRTEM) image and selected area electron diffraction (SAED), as evidenced by no crystal lattice fringe in HRTEM image (Figure 1 f) and no diffraction ring in SAED pattern (Figure 1 g). According to the energy dispersive spectrum (EDS; Supporting Information, Figure S4), the sample consists of Co, S, and O element with Co/S ratio of about 0.76, suggesting that the product is a non-stoichiometric compound.

Electrochemical impedance spectroscopy (EIS) and electrochemical double-layer capacitance (C_{dl}) were measured on the set of samples. As shown in Figure 2 a, the semicircular characteristic of EIS curves indicates that the A-CoS_{4.6}O_{0.6} PNCs have a smaller charge transfer resistance than that of the bulk CoS₂ and the RuO₂. Furthermore, the A-CoS_{4.6}O_{0.6} PNCs show significant enhancement in electrochemical active surface area (ECSA), which is estimated by the double layer capacitance (C_{dl}) calculated by the slope of the linear relationship between the current density against the scan rate. The A-CoS_{4.6}O_{0.6} PNCs present a C_{dl} of 89 mF cm⁻², almost 40 times higher than that of the bulk CoS₂ (2.4 mF cm⁻²) and 4 times higher than that of the RuO₂ (20.4 mF cm⁻²) (Figure 2 b; Supporting Information, Figure S8), implying that the A-CoS_{4.6}O_{0.6} PNCs could expose

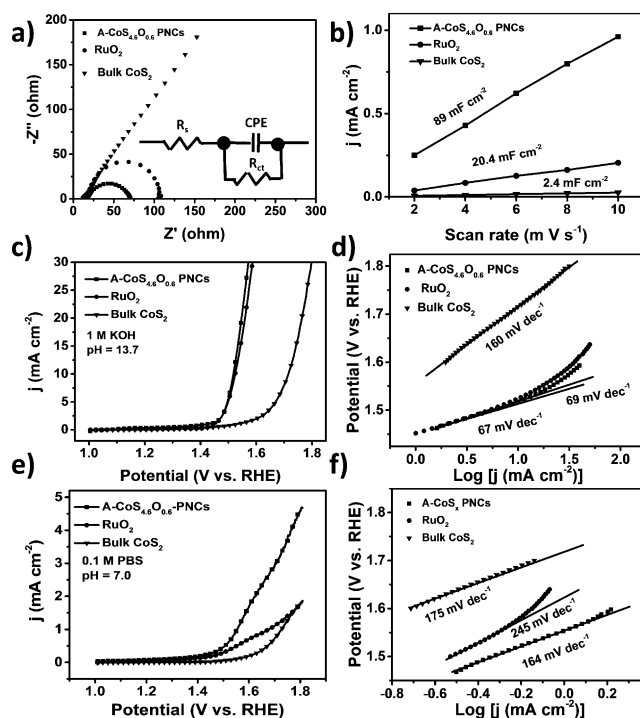


Figure 2. a) EIS recorded at 1.505 V and (inset) corresponding equivalent circuit; b) plots of the current density at 1.23 V vs. the scan rate; c), d) polarization curves and Tafel curves for OER in 1 M KOH (pH 13.7); e), f) Polarization curves and Tafel curves for OER in 0.1 M PBS (pH 7.0) of A-CoS_{4.6}O_{0.6} PNCs, RuO₂, and bulk CoS₂.

more catalytic active sites,^[14] which may be associated with its high Brunauer–Emmett–Teller (BET) surface area (Supporting Information, Figure S5) and enhanced defects originating from ionic exchange reaction.

To evaluate the electrocatalytic activity toward OER, the electrochemical measurements were performed by adopting a typical three-electrode cell setup in 1.0 M KOH (pH 13.7) and 0.1 M phosphate buffer solutions (PBS, pH 7.0), respectively. Figure 2 c, d display linear sweep voltammetry (LSV) curves and Tafel curves of different catalysts in 1.0 M KOH. The A-CoS_{4.6}O_{0.6} PNCs deliver a current density of 10 mA cm⁻² at 1.52 V; this value is slightly lower than that of the RuO₂ (1.53 V) and much lower than that of the bulk CoS₂ (1.71 V). Furthermore, the Tafel slope for the A-CoS_{4.6}O_{0.6} PNCs is 67 mV dec⁻¹ (Figure 2 d), which is also very close to that of the RuO₂ (69 mV dec⁻¹) and much lower than that of the bulk CoS₂ (160 mV dec⁻¹). Further electrochemical tests demonstrate the A-CoS_{4.6}O_{0.6} PNCs proceed a four-electron pathway toward driving OER with excellent stability upon long-term operation (Supporting Information, Figure S9). In fact, the A-CoS_{4.6}O_{0.6} PNCs also show advantages over many other OER catalysts in terms of the major performance parameters (Supporting Information, Table S1). Based on the excellent OER performance in alkaline solution, A home-made Zn-air battery was built with the A-CoS_{4.6}O_{0.6} PNCs as cathode catalyst,^[15] which affords a current density of 10 mA cm⁻² with lowering the charging potential (Supporting Information, Figure S10).

Figure 2 e, f compares electrocatalytic activity of OER at different catalysts in 0.1 M PBS (pH 7.0). The A-CoS_{4.6}O_{0.6}

PNCs display an onset potential of 1.50 V that is very close to that of RuO₂ (1.49 V), whereas exhibit a current density of 4.59 mA cm⁻² at 1.8 V, 2.6 times higher than that of RuO₂. Moreover, the Tafel slope of the A-CoS_{4.6}O_{0.6} PNCs was 164 mV dec⁻¹, significantly lower than that of RuO₂ (245 mV dec⁻¹), manifesting that the A-CoS_{4.6}O_{0.6} PNCs obviously possess much higher catalytic kinetics for OER than RuO₂, which could be further validated by the smaller charge transfer resistance (*R*_{ct}) of A-CoS_{4.6}O_{0.6} PNCs than that of RuO₂ (Supporting Information, Figure S11). Overall, the performance of the A-CoS_{4.6}O_{0.6} PNCs can beat most of the previously reported OER catalysts in neutral solutions (Supporting Information, Table S2).

To further understand the structure–performance relationships, X-ray photoelectron spectroscopy (XPS) and X-ray absorption fine structure spectroscopy (XAFS) were carried out. As shown in Figure 3 a, similar to the bulk CoS₂, the two peaks at about 778.9 eV and 793.9 eV are attributed to the formation of Co-S bands of the A-CoS_{4.6}O_{0.6} PNCs.^[16] And the pair of peaks at 781.6 eV and 797.7 eV belong to the Co–O bond.^[17] Besides, the satellite peaks at 787.2 eV and 803.0 eV are indexed to Co²⁺ ions.^[18] From Figure 3 b, the peaks between 168–172 eV can be attributed to the surface absorption of oxygen with sulfur,^[19] while the binding energy from 161 eV to 166 eV is coordinate with the binding energy of Co–S bonds.^[19,20] The XPS analysis manifests that oxygen is doped into the CoS_x hosts. The X-ray absorption near-edge structure (XANES) has the fingerprint characteristic for identification of the coordination geometry (Figure 3 c).^[17a,21] The spectral shapes of Co K-edge XANES for cobalt oxide

show an intense main peak (the white line peak), while the corresponding peak disappears in the spectrum of cobalt sulfide. Therefore, the XANES spectral shapes of the A-CoS_{4.6}O_{0.6} PNCs are more similar to that of CoS₂ compound, rather than that of CoO compound, indicating the A-CoS_{4.6}O_{0.6} PNCs have an analogous Co–S octahedral structure to the CoS₂. Moreover, the Fourier transform (FT) of extended EXAFS curves of the A-CoS_{4.6}O_{0.6} PNCs show that the average bond length in the first shell was remarkably reduced relative to the Co–S bonds (Figure 3 d), confirming the partial formation of Co–O bonds in the A-CoS_{4.6}O_{0.6} PNCs. The introduction of O atoms around Co center atoms could generate more local disordered structure, as manifested by the significantly decreased intensity beyond the first shell peaks.^[17a,22] To quantitatively obtain the information of coordination atoms, we used the ARTEMIS module of IFEFFIT and USTCXAFS software to perform a least-squares curve parameter fitting.^[23] The best fit of the A-CoS_{4.6}O_{0.6} PNCs octahedron features a Co atom is surrounded by 4.6 S atoms and 0.6 O atoms with formation of plentiful Co–S dangling bonds (Supporting Information, Figure S12 and Table S3).

Density functional theory (DFT) based computation was further performed to determine the role of the incorporated O atom and Co–S dangling bonds. The bulk CoS₂, the CoS₂-vac, the CoS₂-O, and the A-CoS_{4.6}O_{0.6} PNCs were denoted as the bulk of CoS₂ contains no vacancy and O replacement, only vacancy, only O replacement, and both O replacement and vacancy, respectively. The side views are shown in the Supporting Information, Figure S14. Figure 3 e shows the relative activity between the bulk CoS₂ and amorphous CoS₂, it is clear that the A-CoS_{4.6}O_{0.6} PNCs have higher O affinity than the bulk CoS₂, leading to significantly improved activity against CoS₂. To clarify such affinity strengthening effect, the models with only S vacancy and only O replacement are calculated, respectively. It turns out that O replacement can greatly enhancing the O* adsorption. Furthermore, when vacancy was introduced into the situation CoS₂-O, the activity can also be obviously enhanced, as manifested by the relative activities between A-CoS_{4.6}O_{0.6} PNCs and CoS₂-O (Figure 3 e), suggesting that the vacancy sites may act as assistance in strengthening the O* adsorption. Hence, DFT results have proved the A-CoS_{4.6}O_{0.6} PNCs can improve the OER activity by strengthening the O* adsorption benefiting from incorporation of O atoms.

In summary, oxygen-incorporated amorphous cobalt sulfide porous nanocubes were successfully prepared through a galvanic replacement reaction. Systematic studies of electrochemical tests, materials characterization, and DFT calculation, confirmed the following two features in A-CoS_{4.6}O_{0.6} PNCs synergistically contribute to promoting activity for water oxidation in an alkaline/neutral medium: 1) the hollow amorphous structure with ultrafine nanoparticles as building block can expose more active sites with facilitating mass transport at catalytic interface; 2) the Co–S dangling bands and oxygen incorporation into CoS_x host can greatly strengthen the O* adsorption and thus significantly enhance the activity on a single site. The present work not only holds promise for developing an efficient electrocatalyst for water

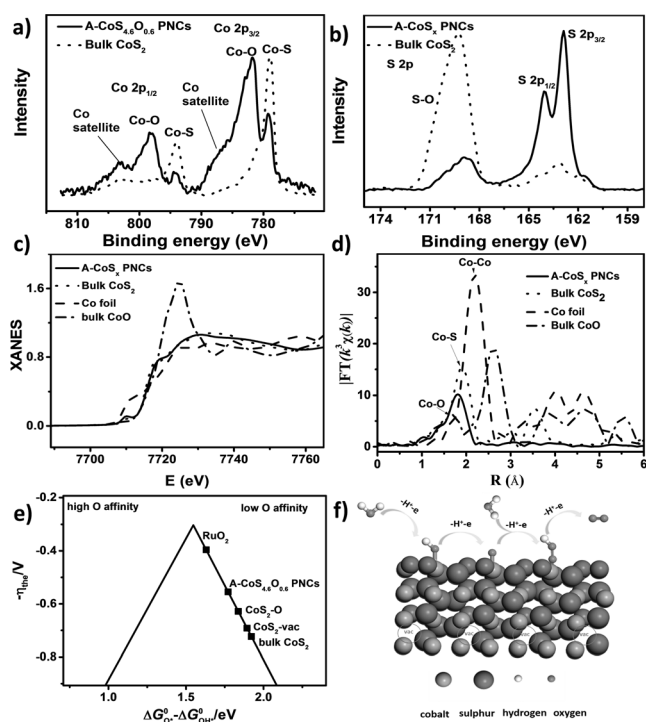


Figure 3. a) High-resolution X-ray photoelectron spectroscopy (XPS) of Co 2p level and b) S 2p level. c) XANES spectra and d) the corresponding FT curves of A-CoS_{4.6}O_{0.6} PNCs, bulk CoS₂, Co foil, and bulk CoO. e) The theoretical volcano plots containing each CoS₂ (001) surface. f) The OER process occurred on the surface of A-CoS_{4.6}O_{0.6} PNCs.

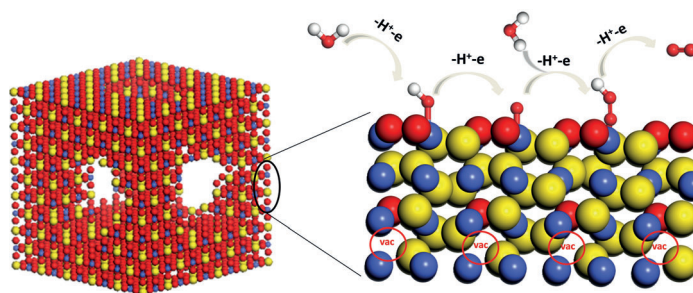
Communications



Electrocatalysis

P. W. Cai, J. H. Huang, J. X. Chen,
Z. H. Wen* ————— ■■■■-■■■■

Oxygen-Incorporated Amorphous Cobalt Sulfide Porous Nanocubes as High-Activity Electrocatalysts for the Oxygen Evolution Reaction in an Alkaline/Neutral Medium



Oxygen incorporated amorphous cobalt sulfide porous nanocubes, benefiting from Co–S dangling bands in the distorted $\text{CoS}_{4.6}\text{O}_{0.6}$ octahedral structure, as well as oxygen incorporation into CoS_x

hosts, show outstanding electrocatalytic activity for water oxidation in alkaline and neutral electrolytes. vac = vacancy; Co blue, S yellow, O red, H white.